

Climbing the Jaynes-Cummings Ladder and Observing its \sqrt{n} Nonlinearity in a Cavity QED System

J. M. Fink,¹ M. Göppl,¹ M. Baur,¹ R. Bianchetti,¹ P. J. Leek,¹ A. Blais,² and A. Wallraff¹

¹*Department of Physics, ETH Zurich, CH-8093, Zurich, Switzerland.*

²*Département de Physique, Université de Sherbrooke, Sherbrooke, Québec, J1K 2R1 Canada.*

(Dated: February 11, 2009)

The already very active field of cavity quantum electrodynamics (QED), traditionally studied in atomic systems [1, 2, 3], has recently gained additional momentum by the advent of experiments with semiconducting [4, 5, 6, 7, 8] and superconducting [9, 10, 11] systems. In these solid state implementations, novel quantum optics experiments are enabled by the possibility to engineer many of the characteristic parameters at will. In cavity QED, the observation of the vacuum Rabi mode splitting is a hallmark experiment aimed at probing the nature of matter-light interaction on the level of a single quantum. However, this effect can, at least in principle, be explained classically as the normal mode splitting of two coupled linear oscillators [12]. It has been suggested that an observation of the scaling of the resonant atom-photon coupling strength in the Jaynes-Cummings energy ladder [13] with the square root of photon number n is sufficient to prove that the system is quantum mechanical in nature [14]. Here we report a direct spectroscopic observation of this characteristic quantum nonlinearity. Measuring the photonic degree of freedom of the coupled system, our measurements provide unambiguous, long sought for spectroscopic evidence for the quantum nature of the resonant atom-field interaction in cavity QED. We explore atom-photon superposition states involving up to two photons, using a spectroscopic pump and probe technique. The experiments have been performed in a circuit QED setup [15], in which ultra strong coupling is realized by the large dipole coupling strength and the long coherence time of a superconducting qubit embedded in a high quality on-chip microwave cavity. Circuit QED systems also provide a natural quantum interface between flying qubits (photons) and stationary qubits for applications in quantum information processing and communication (QIPC) [16].

The dynamics of a two level system coupled to a single mode of an electromagnetic field is described by the Jaynes-Cummings Hamiltonian

$$\hat{\mathcal{H}}_0 = \hbar\omega_{ge}\hat{\sigma}_{ee} + \hbar\omega_r\hat{a}^\dagger\hat{a} + \hbar g_{ge}(\hat{\sigma}_{ge}^\dagger\hat{a} + \hat{a}^\dagger\hat{\sigma}_{ge}). \quad (1)$$

Here, ω_{ge} is the transition frequency between the ground $|g\rangle$ and excited state $|e\rangle$ of the two level system, ω_r is the frequency of the field and g_{ge} is the coupling strength between the two. \hat{a}^\dagger and \hat{a} are the raising and lowering operators acting on the photon number states $|n\rangle$ of the field and $\hat{\sigma}_{ij} = |i\rangle\langle j|$ are the corresponding operators acting on the qubit states. When the coherent coupling rate g_{ge} is larger than the rate κ at which photons are lost from the field and larger than the rate γ at which the two level system loses its coherence, the strong coupling limit is realized. On resonance ($\omega_{ge} = \omega_r$) and in the presence of n excitations, the new eigenstates of the coupled system are the symmetric $(|g, n\rangle + |e, n-1\rangle)/\sqrt{2} \equiv |n+\rangle$ and antisymmetric $(|g, n\rangle - |e, n-1\rangle)/\sqrt{2} \equiv |n-\rangle$ qubit-photon superposition states, see Fig. 1. For $n = 1$, these states are equivalently observed spectroscopically as a vacuum Rabi mode splitting [4, 5, 6, 7, 8, 9, 17, 18] or in time resolved measurements as vacuum Rabi oscillations [11, 19, 20, 21] at frequency $2g_{ge}$. The Jaynes-Cummings model predicts a characteristic nonlinear scaling of this frequency as $\sqrt{n}g_{ge}$ with the number of excitations n in

the system, see Fig. 1. This quantum effect is in stark contrast to the normal mode splitting of two classical coupled linear oscillators, which is independent of the oscillator amplitude.

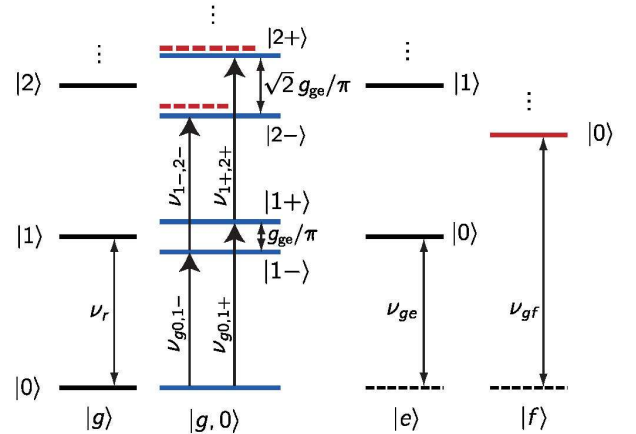


Fig. 1: **Level diagram of a resonant ($\nu_r = \nu_{ge}$) cavity QED system.** The uncoupled qubit states $|g\rangle, |e\rangle$ and $|f\rangle$ from left to right and the photon states $|0\rangle, |1\rangle, \dots, |n\rangle$ from bottom to top are shown. The dipole coupled dressed states are shown in blue and a shift due to the $|f, 0\rangle$ level is indicated in red. Pump $\nu_{g0,1-}$, $\nu_{g0,1+}$ and probe $\nu_{1-,2-}$, $\nu_{1+,2+}$ transition frequencies are indicated accordingly.

Since the first measurements of the vacuum Rabi mode splitting with, on average, a single intra-cavity atom [17] it remains a major goal to clearly observe this characteristic \sqrt{n} nonlinearity spectroscopically to prove the quantum nature of the interaction between the two-level system and the radiation field [12, 14, 22]. In time domain measurements of vacuum Rabi oscillations, evidence for this \sqrt{n} scaling has been found with circular Rydberg atoms [19] and superconducting flux qubits [11] interacting with weak coherent fields. Related experiments have been performed with one and two-photon Fock states [20, 21]. We now observe this nonlinearity directly using a scheme similar to the one suggested in Ref. [22] by pumping the system selectively into the first doublet $|1\pm\rangle$ and probing transitions to the second doublet $|2\pm\rangle$. This technique realizes efficient excitation into higher doublets at small intra cavity photon numbers avoiding unwanted a.c. Stark shifts occurring in high drive and elevated temperature experiments.

In a different regime, when the qubit is detuned by an amount $|\Delta| = |\omega_{ge} - \omega_r| \gg g_{ge}$ from the cavity, photon number states and their distribution have recently been observed using dispersive quantum non-demolition measurements in both circuit QED [23] and Rydberg atom experiments [24].

In our experiments, in the resonant regime a superconducting qubit playing the role of an artificial atom is strongly coupled to photons contained in a coplanar waveguide resonator in an architecture known as circuit QED [9, 15]. We use a transmon [25, 26], which is a charge-insensitive superconducting qubit design derived from the Cooper pair box (CPB) [27], as the artificial atom. Its transition frequency is given by $\omega_{ge}/2\pi \simeq \sqrt{8E_C E_J(\Phi)}$ with the single electron charging energy $E_C \approx 0.4$ GHz, the flux controlled Josephson energy $E_J(\Phi) = E_{J,\max} |\cos(\pi\Phi/\Phi_0)|$ and $E_{J,\max} \approx 53.5$ GHz, as determined in spectroscopic measurements. The cavity is realized as a coplanar resonator with bare resonance frequency $\nu_r \approx 6.94$ GHz and decay rate $\kappa/2\pi \approx 0.9$ MHz. Optical images of the sample are shown in Fig. 2a. The large dimension of the qubit in the quasi one dimensional resonator layout provides a very large dipole coupling strength g_{ge} . A simplified electrical circuit diagram of the setup is shown in Fig. 2b.

The system is prepared in its ground state $|g, 0\rangle$ by cooling it to temperatures below 20 mK in a dilution refrigerator. We then probe the energies of the lowest doublet $|1\pm\rangle$ measuring the cavity transmission spectrum T and varying the detuning between the qubit transition frequency ν_{ge} and the cavity frequency ν_r by applying a magnetic flux Φ , see Fig. 3a. The measurement is performed with a weak probe of power $P \approx -137$ dBm applied to the input port of the resonator populating it with a mean photon number of $\bar{n} \approx 1.6$ on resonance when the qubit is maximally detuned from the resonator. P is calibrated in a dispersive a.c. Stark shift measure-

ment [28]. At half integers of a flux quantum Φ_0 , the qubit energy level separation ν_{ge} approaches zero. At this point the bare resonator spectrum peaked at the frequency ν_r is observed, see Fig. 3b. We use the measured maximum transmission amplitude to normalize the amplitudes in all subsequent measurements. At all other detunings $|\Delta| \gg g_{ge}$ the qubit dispersively shifts [25] the cavity frequency ν_r by $\chi \simeq -g_{ge}^2 E_C / (\Delta(\Delta - E_C))$.

Measuring cavity transmission T as a function of flux bias Φ in the anti-crossing region yields transmission maxima at frequencies corresponding to transitions to the first doublet $|1\pm\rangle$ in the Jaynes-Cummings ladder as shown in Fig. 3c. On resonance ($\Delta = 0$), we extract a coupling strength of $g_{ge}/2\pi = 154$ MHz, see Fig. 3d, where the linewidth of the individual vacuum Rabi split lines is given by $\delta_{\nu 0} \approx 2.6$ MHz. This corresponds to a transmission peak separation g_{ge}/π of over 100 linewidths $\delta_{\nu 0}$, clearly demonstrating that the strong coupling limit is realized [9, 29]. Solid white lines in Figs. 3 (and 4) are numerically calculated dressed state frequencies with the qubit and resonator parameters as stated above, being in excellent agreement with the data. For the calculation, the qubit Hamiltonian is solved exactly in the charge basis. The qubit states $|g\rangle$ and $|e\rangle$ and the flux

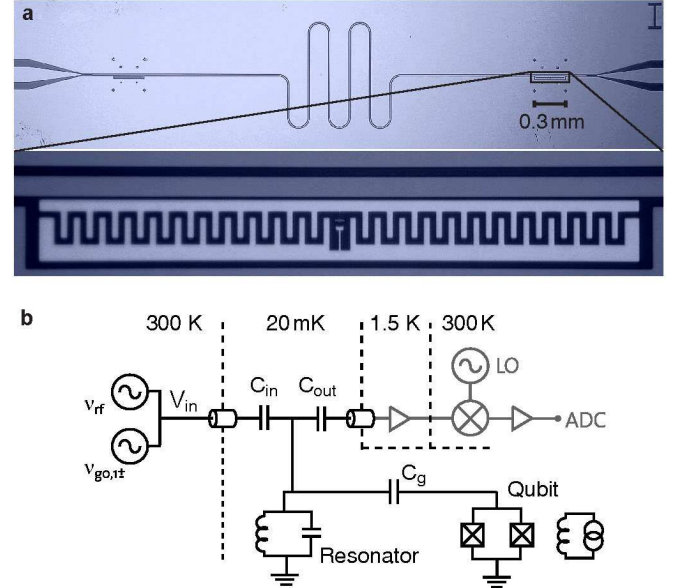


Fig. 2: Sample and experimental setup. **a**, Optical images of the superconducting coplanar waveguide resonator (top) with the transmon type superconducting qubit embedded at the position indicated. On the bottom, the qubit with dimensions $300 \times 30 \mu\text{m}^2$ close to the center conductor is shown. **b**, Simplified circuit diagram of the experimental setup, similar to the one used in Ref. [9]. The qubit is capacitively coupled to the resonator through C_g and the resonator, represented by a parallel LC circuit, is coupled to input and output transmission lines via the capacitors C_{in} and C_{out} . Using ultra low noise amplifiers and a down-conversion mixer, the transmitted microwave signal is detected and digitized.

dependent coupling constant g_{ge} are then incorporated in the Jaynes-Cummings Hamiltonian Eq. (1). Its numeric diagonalization yields the dressed states of the coupled system without any fit parameters.

In our pump and probe scheme we first determine the exact energies of the first doublet $|1\pm\rangle$ at a given flux Φ spectroscopically. We then apply a pump tone at the fixed frequency $\nu_{g0,1-}$ or $\nu_{g0,1+}$ to populate the respective first doublet state $|1\pm\rangle$. A probe tone of the same power is then scanned over the frequency range of the splitting. This procedure is repeated for different flux controlled detunings. The transmission at the pump and probe frequencies is spectrally resolved in a heterodyne detection scheme.

Populating the symmetric state $|1+\rangle$, we observe an additional transmission peak at a probe tone frequency that varies with flux, as shown in Fig. 4a. This peak corresponds to the transition between the symmetric doublet states $|1+\rangle$ and $|2+\rangle$ at frequency $\nu_{1+,2+}$. Similarly, in Fig. 4c where the antisymmetric state $|1-\rangle$ is populated we measure a transmission peak that corresponds to the transition between the two antisymmetric doublet

states $|1-\rangle$ and $|2-\rangle$ at frequency $\nu_{1-,2-}$. The transmission spectra displayed in Figs. 4b and d recorded at the values of flux indicated by arrows in Figs. 4a and c show that the distinct transitions between the different doublets are very well resolved with separations of tens of linewidths. Transitions between symmetric and antisymmetric doublet states are not observed in this experiment, because the flux-dependent transition matrix elements squared are on average smaller by a factor of 10 and 100 for transitions $|1+\rangle \rightarrow |2-\rangle$ and $|1-\rangle \rightarrow |2+\rangle$, respectively, than the corresponding matrix elements between states of the same symmetry.

The energies of the first doublet $|1\pm\rangle$, split by g_{ge}/π on resonance, are in excellent agreement with the dressed states theory (solid red lines) over the full range of flux Φ controlled detunings, see Fig. 5. The absolute energies of the second doublet states $|2\pm\rangle$ are obtained by adding the extracted probe tone frequencies $\nu_{1-,2-}$ and $\nu_{1+,2+}$ to the applied pump frequencies $\nu_{g0,1-}$ or $\nu_{g0,1+}$, see blue dots in Fig. 5. For the second doublet, we observe two peaks split by $1.34 g_{ge}/\pi$ on resonance, a value very close to the expected $\sqrt{2} \sim 1.41$. This small frequency shift can easily be understood, without any fit parameters, by taking into account a third qubit level $|f, 0\rangle$ which is at

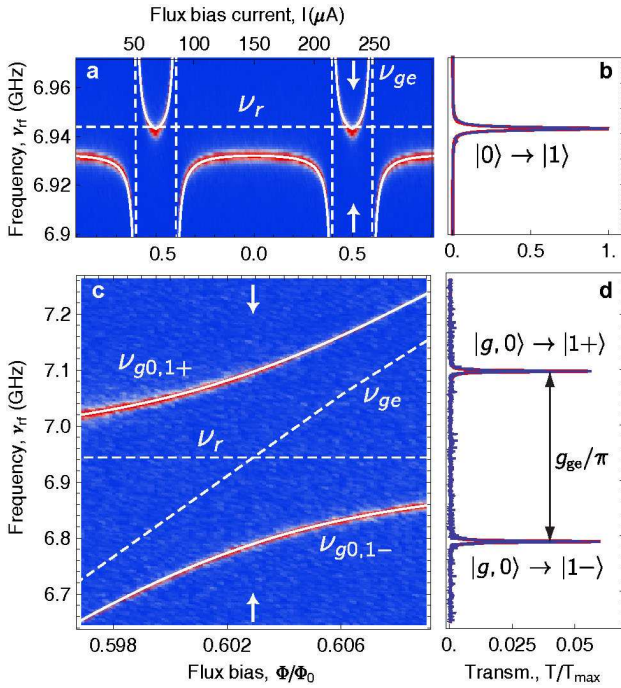


Fig. 3: Vacuum Rabi mode splitting with a single photon. **a**, Measured resonator transmission spectra versus external flux Φ . Blue indicates low and red high transmission T . The solid white line shows dressed state energies as obtained numerically and the dashed lines indicate the bare resonator frequency ν_r as well as the qubit transition frequency ν_{ge} . **b**, Resonator transmission T at $\Phi/\Phi_0 = 1/2$ as indicated with arrows in panel **a**, with a Lorentzian line fit in red. **c**, Resonator transmission T versus Φ close to degeneracy. **d**, Vacuum Rabi mode splitting at degeneracy with Lorentzian line fit in red.

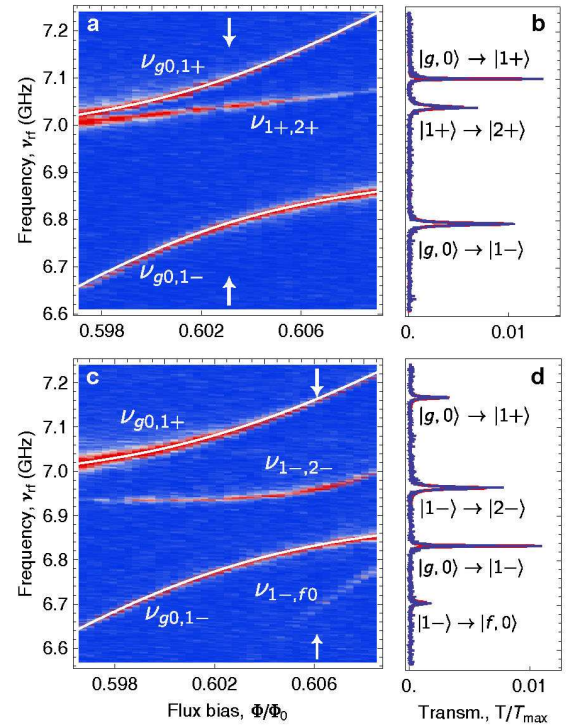


Fig. 4: Vacuum Rabi mode splitting with two photons. **a**, Cavity transmission T as in Fig. 3 with an additional pump tone applied to the resonator input at frequency $\nu_{g0,1+}$ populating the $|1+\rangle$ state. **b**, Spectrum at $\Delta = 0$, indicated by arrows in **a**. **c**, Transmission T with a pump tone applied at $\nu_{g0,1-}$ populating the $|1-\rangle$ state. **d**, Spectrum at $\Phi/\Phi_0 \approx 0.606$ as indicated by arrows in **c**.

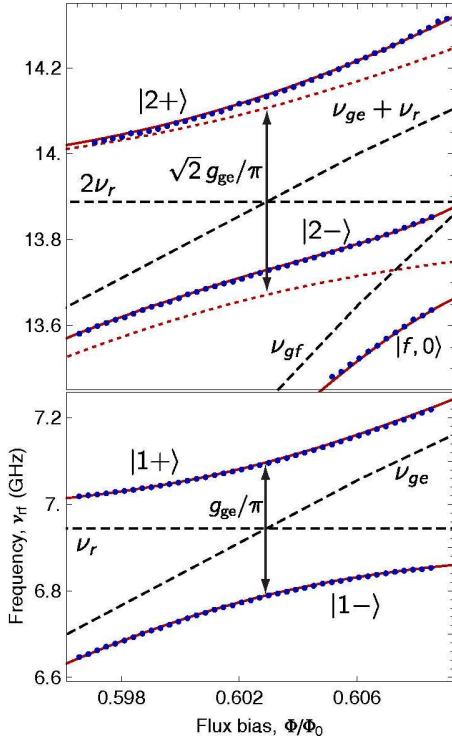


Fig. 5: **Experimental dressed state energy levels.** Measured dressed state energies (blue dots) reconstructed by summing pump and probe frequencies, compared to the calculated uncoupled cavity and qubit levels (dashed lines), the calculated dressed state energies in the qubit two-level approximation (dotted) and to the corresponding calculation including the third qubit level (solid red lines).

frequency $\nu_{gf} \simeq 2\nu_{ge} - E_C$ for the transmon type qubit [25], just below the second doublet states $|2\pm\rangle$. In order to find the energies of the dressed states in the presence of this additional level we diagonalize the Hamiltonian $\hat{\mathcal{H}} = \hat{\mathcal{H}}_0 + \hat{\mathcal{H}}_1$, where $\hat{\mathcal{H}}_1 = \hbar\omega_{gf}\hat{\sigma}_{ff} + \hbar g_{ef}(\hat{\sigma}_{ef}^\dagger\hat{a} + \hat{a}^\dagger\hat{\sigma}_{ef})$ and $g_{ef}/2\pi \approx 210$ MHz (obtained from exact diagonalization) denotes the coupling of the $|e\rangle$ to $|f\rangle$ transition to the cavity. The presence of the $|f, 0\rangle$ level is observed to shift the antisymmetric state $|2-\rangle$, being closer in frequency to the $|f, 0\rangle$ state, more than the symmetric state $|2+\rangle$, see Figs. 1 and 5, leading to the small difference of the observed splitting from $\sqrt{2}$. The $|f, 0\rangle$ state, being dressed by the states $|g, 2\rangle$ and $|e, 1\rangle$, is also directly observed in the spectrum via the transition $|1-\rangle \rightarrow |f, 0\rangle$ at frequency $\nu_{1-,f0}$, see Fig. 4c. This is in excellent agreement with the dressed states model, see Fig. 5. For comparison the dressed states split by $\sqrt{2}g_{ge}/\pi$ in the absence of the $|f, 0\rangle$ state are shown as dotted red lines in Fig. 5.

Our experiments clearly demonstrate the quantum non-linearity of a system of one or two photons strongly coupled to a single artificial atom in a cavity QED setting. Both symmetric and antisymmetric superposition states involving up to two photons are resolved by many

tens of linewidths. Recently, signatures of the $|2-\rangle$ state have also been observed spectroscopically in an independent work on optical cavity QED [30]. We have also observed that higher excited states of the artificial atom can induce energy shifts in the coupled atom-photon states. These shifts should also be observable in time resolved measurements of Rabi-oscillations with photon number states. In this circuit QED system, excited states $|n\pm\rangle$ with $n > 2$ are also observable both by pumping the system with thermal photons and by applying strong coherent drive fields inducing multi-photon transitions. The observed very strong nonlinearity on the level of single or few quanta could be used for the realization of a single photon transistor, parametric down-conversion, and for the generation and detection of individual microwave photons.

We thank L. S. Bishop, J. M. Chow, T. Esslinger, L. Frunzio, A. Imamoglu, B. R. Johnson, Jens Koch, R. J. Schoelkopf and D. I. Schuster for valuable discussions. This work was supported by SNF and ETHZ. P. J. L. was supported by the EU with a MC-EIF. A. B. was supported by NSERC, CIFAR and FQRNT.

-
- [1] Raimond, J. M., Brune, M., & Haroche, S. Manipulating quantum entanglement with atoms and photons in a cavity. *Rev. Mod. Phys.* **73**(3), 565–582 (2001).
 - [2] Mabuchi, H. & Doherty, A. C. Cavity Quantum Electrodynamics: Coherence in Context. *Science* **298**(5597), 1372–1377 (2002).
 - [3] Walther, H., Varcoe, B. T. H., Englert, B.-G., & Becker, T. Cavity quantum electrodynamics. *Rep. Prog. Phys.* **69**(5), 1325–1382 (2006).
 - [4] Reithmaier, J. P. *et al.* Strong coupling in a single quantum dot-semiconductor microcavity system. *Nature* **432**(7014), 197–200 (2004).
 - [5] Yoshie, T. *et al.* Vacuum Rabi splitting with a single quantum dot in a photonic crystal nanocavity. *Nature* **432**(7014), 200–203 (2004).
 - [6] Peter, E. *et al.* Exciton-photon strong-coupling regime for a single quantum dot embedded in a microcavity. *Phys. Rev. Lett.* **95**(6), 067401 (2005).
 - [7] Hennessy, K. *et al.* Quantum nature of a strongly coupled single quantum dot-cavity system. *Nature* **445**(7130), 896–899 (2007).
 - [8] Englund, D. *et al.* Controlling cavity reflectivity with a single quantum dot. *Nature* **450**(7171), 857–861 (2007).
 - [9] Wallraff, A. *et al.* Strong coupling of a single photon to a superconducting qubit using circuit quantum electrodynamics. *Nature* **431**, 162–167 (2004).
 - [10] Chiorescu, I. *et al.* Coherent dynamics of a flux qubit coupled to a harmonic oscillator. *Nature* **431**(7005), 159–162 (2004).
 - [11] Johansson, J. *et al.* Vacuum Rabi oscillations in a macroscopic superconducting qubit LC oscillator system. *Phys. Rev. Lett.* **96**(12), 127006 (2006).
 - [12] Zhu, Y. *et al.* Vacuum Rabi splitting as a feature of linear-dispersion theory: Analysis and experimental ob-

- servations. *Phys. Rev. Lett.* **64**(21), 2499–2502 (1990).
- [13] Walls, D. & Milburn, G. *Quantum optics*. (Springer-Verlag, Berlin, 1994).
- [14] Carmichael, H. J., Kochan, P., & Sanders, B. C. Photon correlation spectroscopy. *Phys. Rev. Lett.* **77**(4), 631–634 (1996).
- [15] Blais, A., Huang, R. S., Wallraff, A., Girvin, S. M., & Schoelkopf, R. J. Cavity quantum electrodynamics for superconducting electrical circuits: An architecture for quantum computation. *Phys. Rev. A* **69**(6), 062320 (2004).
- [16] Nielsen, M. A. & Chuang, I. L. *Quantum Computation and Quantum Information*. (Cambridge University Press, Cambridge, 2000).
- [17] Thompson, R. J., Rempe, G., & Kimble, H. J. Observation of normal-mode splitting for an atom in an optical cavity. *Phys. Rev. Lett.* **68**(8), 1132–1135 (1992).
- [18] Boca, A. *et al.* Observation of the vacuum Rabi spectrum for one trapped atom. *Phys. Rev. Lett.* **93**(23), 233603 (2004).
- [19] Brune, M. *et al.* Quantum Rabi oscillation: A direct test of field quantization in a cavity. *Phys. Rev. Lett.* **76**(11), 1800–1803 (1996).
- [20] Varcoe, B. T. H., Brattke, S., Weidinger, M., & Walther, H. Preparing pure photon number states of the radiation field. *Nature* **403**(6771), 743–746 (2000).
- [21] Bertet, P. *et al.* Generating and probing a two-photon fock state with a single atom in a cavity. *Phys. Rev. Lett.* **88**(14), 143601 (2002).
- [22] Thompson, R. J., Turchette, Q. A., Carnal, O., Kimble, H. J. Nonlinear spectroscopy in the strong-coupling regime of cavity QED. *Phys. Rev. A* **57**(4), 3084–3104 (1998).
- [23] Schuster, D. I. *et al.* Resolving photon number states in a superconducting circuit. *Nature* **445**(7127), 515–518 (2007).
- [24] Guerlin, C. *et al.* Progressive field-state collapse and quantum non-demolition photon counting. *Nature* **448**(7156), 889–893 (2007).
- [25] Koch, J. *et al.* Charge-insensitive qubit design derived from the Cooper pair box. *Phys. Rev. A* **76**(4), 042319 (2007).
- [26] Schreier, J. A. *et al.* Suppressing charge noise decoherence in superconducting charge qubits. *Phys. Rev. B* **77**, 180502(R) (2008).
- [27] Bouchiat, V., Vion, D., Joyez, P., Esteve, D., & Devoret, M. H. Quantum coherence with a single Cooper pair. *Phys. Scr.* **T76**, 165–170 (1998).
- [28] Schuster, D. I. *et al.* AC Stark shift and dephasing of a superconducting qubit strongly coupled to a cavity field. *Phys. Rev. Lett.* **94**(12), 123602 (2005).
- [29] Schoelkopf, R. J. & Girvin, S. M. Wiring up quantum systems. *Nature* **451**, 664669 (2008).
- [30] Schuster, I. *et al.* Nonlinear spectroscopy of photons bound to one atom. *Nat. Phys.* **4**(5), 382–385 (2008).